geographies

MDPI

Article

Assessing the Coastal Vulnerability by Combining Field Surveys and the Analytical Potential of CoastSat in a Highly Impacted Tourist Destination

Luis Valderrama-Landeros [1], Francisco Flores-Verdugo [2] and Francisco Flores-de-Santiago [3,*]

[1] Subcoordinación de Percepción Remota, Comisión Nacional para el Conocimiento y uso de la Biodiversidad (CONABIO), 4903 Liga Periférico-Insurgentes Sur, Tlalpan, Mexico City 14010, Mexico
[2] Instituto de Ciencias del Mar y Limnología, Unidad Académica Mazatlán, Universidad Nacional Autónoma de México, Av. Joel Montes Camarena s/n, Mazatlán 82040, Mexico
[3] Instituto de Ciencias del Mar y Limnología, Unidad Académica Procesos Oceánicos y Costeros, Universidad Nacional Autónoma de México, A.P. 70-305, Av. Universidad 3000, CU, Mexico City 04510, Mexico
* Correspondence: ffloresd@cmarl.unam.mx

Abstract: Tropical sandy beaches provide essential ecosystem services and support many local economies. In recent times, however, there has been a massive infrastructure expansion in popular tourist destinations worldwide. To investigate the shoreline variability at a popular tourist destination in Mexico, we used the novel semi-automatic CoastSat program (1980 to 2020) and the climate dataset ERA5 (wave energy and direction). We also measured the beach cross-shore distance and the foredune height with topographic surveys. The results indicate that the section of real estate seafront infrastructure in the study site presents a considerable shoreline erosion due to the fragmentation between the foredune ridge and the beach berm, based on the in situ transects. Moreover, foredune corridors with cross-shore distances of up to 70 to 90 m and dune heights of 8 m, can be seen in the short unobstructed passages between buildings. In the south section we found the coastline in a much more stable condition because this area has not had coastal infrastructures, as of yet. For the most part, the remote sensing analysis indicates constant erosion since 1990 in the real estate section (mainly seafront hotels) and an overall accretion pattern at the unobstructed beach-dune locations. This study demonstrates the catastrophic consequences of beach fragmentation due to unplanned real estate developments, by combining in situ surveys and a freely available big-data approach (CoastSat).

Keywords: Google Earth Engine; Landsat; Sentinel-2; Mexico

Citation: Valderrama-Landeros, L.; Flores-Verdugo, F.; Flores-de-Santiago, F. Assessing the Coastal Vulnerability by Combining Field Surveys and the Analytical Potential of CoastSat in a Highly Impacted Tourist Destination. *Geographies* **2022**, *2*, 642–656. https://doi.org/10.3390/geographies2040039

Academic Editor: Xu Chen

Received: 31 August 2022
Accepted: 8 October 2022
Published: 21 October 2022

1. Introduction

Although the extension of coastal zones—areas less than 10 m above sea level—represents a small fraction (~2%) of the world (i.e., 1.6 million km), they are home to almost half of the world's human inhabitants, with a much higher population density than in inland areas [1]. The location of nearly two-thirds of worldwide megacities is found within 60 km of the coastlines, representing an enormous economic value for commercial activities, such as maritime transportation, fisheries, and tourism [2]. For instance, 80–90% of the global trade within these cities is carried out in harbors [3]. Moreover, by 2030, the coastal economy will grow to nearly three trillion US dollars, with considerable contributions from harbor activities and international tourism. Despite their economic relevance, current estimates suggest that coastal populations will become increasingly dense, and this will inevitably aggravate the vulnerability to anthropogenic impacts on coastal areas if proper management and law enforcement are not encouraged [4]. So far, the most common human repercussions on coastal regions have been poor land-use planning, e.g., coastal development projects [5] and geomorphological alterations [6], which have ultimately led to habitat degradation.

Furthermore, natural events, such as hurricanes, tsunamis, storm surges, and the persistent sea-level rise, will eventually exacerbate the negative consequences of anthropogenic activities on coastal regions (e.g., beach erosion, increase in the inundation area, and ecosystem degradation) [7].

Open sandy coasts are dynamic environments comprising up to 40% of the length of the global coastal zone. As expected, this type of shoreline is essential for the tourist industry, especially in tropical and subtropical locations [8]. Physical processes such as waves, littoral currents, storm surges, and wind stress influence sandy coasts due to geomorphology. At the very least, these factors modify the sediment distribution and thus affect the geomorphological structure of the shoreline [9]. For instance, foredunes (i.e., longitudinal sand formations) are a standard indicator of the amount of sand accumulation on the beach, making these coastal features essential for beach preservation, as they provide constant sand transportation and prevent erosion [10]. However, coastal infrastructure projects, such as real estate seafront developments, tend to be built on foredunes, setting off sandy beach erosion due to beach fragmentation. Consequently, the coastline retreat is a growing threat of global interest since it affects numerous urbanized beaches where real estate is of high purchasing power, and buildings face the danger of collapse [1]. It has been estimated that up to 70% of sandy beaches worldwide show a degree of continuous erosion. These erosion rates will likely increase, considering the projected variations in the sea level rise and storm surge intensity [11].

Given the problems associated with the coastline infrastructure, protection structures along coastlines are a common approach to diminish erosion and flooding [12]. However, these artificial defensive structures, such as breakwaters (shore-parallel), seawalls, and groins (shore-perpendicular), usually cause even more damage to the surrounding areas [9]. For instance, coastal constructions in front of resorts (seawalls) act as a barrier that inhibits sediment transport and thus leads to narrower beaches with a steeper slope, ultimately causing massive erosion [13]. Another aspect with tremendous implications for these defensive structures is the coastal hydrodynamics involved, such as wave refraction and currents [7]. For instance, groins abduct sediment transported along the coastline, thus affecting beach extension and sand distribution, i.e., erosion on one side and accretion on the other. Conversely, breakwaters decrease wave energy and tend to increase sand deposition. Overall, the collapse of coastal infrastructures is a consequence that was induced by the inadequate planning of coastal land use in the past, mainly owing to the lack of scientific knowledge regarding coastal hydrodynamics and sediment transport, which will eventually cause the complete loss of the recreational value of sandy beaches [14].

To deal with these problems, monitoring, understanding, and predicting coastline dynamics are of vital interest to the public and private sectors [15]. There are two ways to detect the morphological changes in the beach: (i) using topographic techniques in the field and (ii) analyzing the change rates of the coastline, by means of remote sensing and geographic information systems (GIS) [16]. Advancements in field topographic techniques have facilitated the task of monitoring beaches; however, these in situ methods still require trained personnel and are both time-consuming and expensive [17]. Still, if available, they produce data with a higher accuracy. Nonetheless, the salty atmospheric environment caused by waves often produces irreparable failures in electronic instruments in the field [18]. Moreover, in areas where windy conditions are the norm, the sandy beaches of volcanic formations generally have magnetic minerals in the sand, which damage the electrical system or even negatively affect the data recording. Furthermore, previous studies and on-site measurements have been non-existent or unavailable to the public in most tourist destinations with a considerable real estate value (hotels, resorts, etc.). So, the question of when the coastal erosion process began, in most scenarios, has not been fully answered.

The use of cost-effective remote sensing technologies could overcome these limitations by enabling the systematic and global study of coastal areas under adverse environmental conditions [19]. Remote sensing archives could thus provide an effective tool for assessing

how coastal geomorphology was in the past. Over the last decades, a considerable number of research studies have monitored sandy beaches with data from remote sensors [18]. Satellite platforms can effectively monitor the coastal zone globally because each image can cover large areas with an acceptable spatial resolution. In addition, remote sensing data could calculate shoreline change rates by overlapping the multi-temporal data, due to their worldwide digital access. For instance, the Landsat program, launched in 1972, has been the longest-running space mission to acquire satellite images of the earth's surface [20]. Yet the detection of the shoreline position may be affected by uncertainties, such as the tidal range during image acquisition and sensor spatial resolution [21].

We hypothesized that the cross-shore distance and dune height from the field survey are directly related to the accretion and erosion patterns derived from the historical semiautomatic analysis of CoastSat data. We tested this hypothesis by studying a multi-decadal analysis of the coastline variability between a conservation area and a real estate seafront development zone, by means of topographic surveys, remote sensing data, novel cloud computing software, and GIS techniques.

2. Materials and Methods

2.1. Study Area

Mexico is a country with a coastal extension of ~12,000 km, covering the Pacific and Atlantic oceans. Such extension, which includes the unique Gulf of California and the Caribbean Sea, has allowed the development of a widespread network of coastal tourist destinations, such as Cabo San Lucas, Puerto Vallarta, and Cancun. Mexico is currently listed among the top eight places by tourist arrivals, representing a net 9% of the national GDP [22]. However, it is common to find uncontrolled seafront real estate expansions with catastrophic implications for the environment [23]. The city of Mazatlan is a traditional and cultural destination located along the Pacific coast of Mexico on an alluvial plain in the state of Sinaloa (Figure 1). The climate is hot semiarid (BSh), with a mean annual air temperature ranging from 24 to 28 °C and a total precipitation between 900 to 1300 mm [22]. Mazatlan has approximately 24 km of sandy beach deposits, and the local tide is semidiurnal with a maximum amplitude of 1.8 m. The environmental conditions represent the main coastal tourist attraction, reflected in an overwhelming 48% of the city's GDP [23]. Mazatlan has a population of a little over 500,000 inhabitants and an official infrastructure of 181 hotels [22]. Mazatlan, as well as many other touristic destinations in Mexico, presents many challenges regarding environmental conservation. For instance, there has been little interest in conserving natural areas, such as the mangrove forests and the coastal foredune vegetation, to prioritize urbanization. The implications of the uncontrolled constructions commonly found on the beach are severe, as they decrease the coastal ecosystem services.

2.2. Beach Profiles Survey

We divided the coastline of Mazatlan into four sections (Figure 1). From north to south, the first section (red) corresponds to the area from the Cerritos Beach to the marina, with its sparse seafront resorts. The green circles depict a heavily dense area surrounded by real estate seafront buildings. The purple circles indicated the Mazatlan bay section, characterized by a long concrete oceanfront corridor constructed on top of the original foredune without seafront resorts. Finally, the southern region (yellow) has a minor infrastructure along the first two km from the harbor entrance. From this point on, most of the sandy beach does not have any coastal infrastructure until the last section, where there is a major seafront resort. However, due to its attractiveness regarding the beach extension and the closer connection with the international airport, future real estate projects are now being considered for this section of the Mazatlan shoreline.

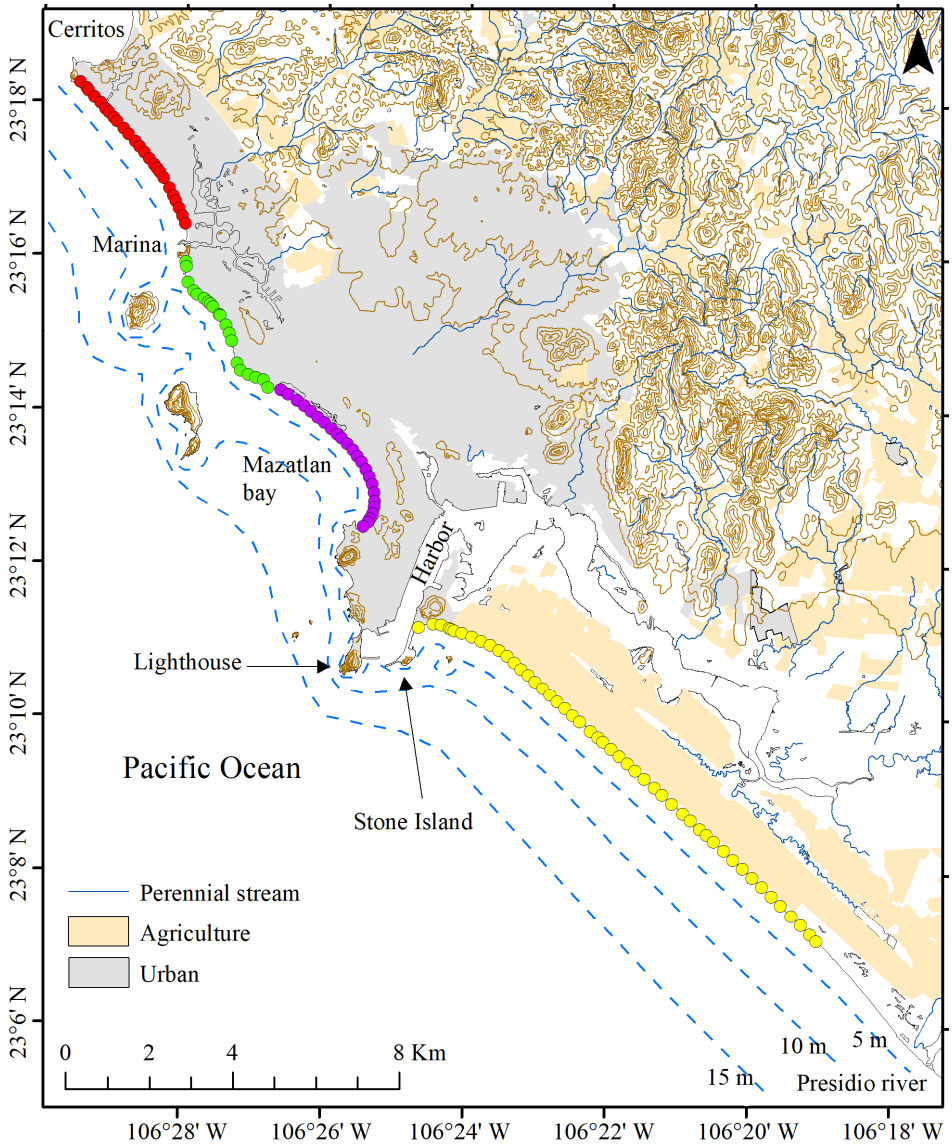

Figure 1. Location of the touristic port of the Mazatlan coastline, Pacific coast of Mexico. The small colored circles indicate the location of the on-site transects: Northern point with non-continuous buildings (red), continuous resorts with no direct access to the beach (green), concrete oceanfront corridor with no constructions in front of the beach (purple), and conserved area without coastal infrastructure (yellow). The brown contour lines indicate the elevation intervals at every 50 m. The dashed lines indicate the bathymetry at depths of 5, 10, and 15 m.

The northern section of the study area (red, green, and purple circles) has an extension of 13.4 km, while the southern one (yellow circles) is 12.5 km long. During the harbor construction, the two islands at the entrance (Stone Island and the natural lighthouse) were connected with breakwaters (~1 km long by ~100 m wide). These breakwaters act as sediment traps and do not allow a connection between both sections of the coasts.

In each area, we measured the cross-shore distance and dune height at every 200 m by means of a STABILA LD 420 laser distance meter, topographic levels, and 10-m high folding staffs [10]. In some situations, it was not possible to obtain profiles at every 200 m due to the large stretches of completely eroded beach. Hence, the loss of electronic equipment was very likely because of the direct impact of the waves on the walls of the hotels.

2.3. Remote Sensing Data Obtention and Image Analysis

We obtained historical shoreline positions by using CoastSat, which is a more objective, robust, and repeatable toolbox in Phyton, developed by Vos et al. [24], to improve the shoreline detection from the satellite image collections of Landsat-5 (1986–2010), -8 (2015), and Sentinel-2 (2020), available on the Google Earth Engine platform. The CoastSat toolbox provides a classification algorithm based on neural networks specializing in separating water, white water, and sand. As a matter of fact, CoastSat allows a better discrimination of elements that can generate false identifications, such as the interface between land and sea [25]. This method allows the user to explore the catalogs of Landsat and Sentinel images and select those considered suitable for extracting coastlines with a sub-pixel resolution technique. In addition, we performed a visual review to avoid including other irrelevant features in case they were present in the images.

CoastSat creates user-defined transects with start-end coordinates, or by drawing them manually, to appreciate the variations in the positions of the lines over time. However, we did not use this module and resorted to the Digital Shore Analysis System tool (DSAS) instead to provide robustness for a systematic analysis along the entire length of the coastline.

We stored the obtained coastline data into a pkl file, which included the coordinates, dates, the RMSE (geometric residuals in the transverse and longitudinal directions), and cloudiness. CoastSat provides the RMSE from the Tiers 1 collection, by combining the geometric residuals in the transverse and longitudinal directions with the ground control points and digital elevation models to correct for displacements. We also created a geometric representation in the geojson format to visualize any geographic information system. We used the first two CoastSat components for both the north and south sections, to extract the coastlines, on an every-five-year basis, from the oldest available date (1986) until June 2020 (Table S1). The estimated mean sea level was determined using the semi-diurnal M2 tidal amplitude harmonic from freely available software (http://predmar.cicese.mx/programa/ accessed on 25 March 2021). The date and time of each satellite image were corrected using GMT-7 from the Mazatlan tidal station.

In as much as the objective was to identify the long-term processes (34 years) and reduce the biases due to effects such as tides or errors in identifying coastlines, we decided to work with the idea of average lines. For each set of lines (Table S1) in a given year, we obtained its average position using the v.centerline.py module implemented in the GRASS software [26]. This step was not possible in the case of the 1986 image in the northern section because only a single useful image was available. Based on the averaged coastlines, we carried out a segmented analysis in different periods (1986–1990, 1990–1995, 1995–2000, 2000–2005, 2005–2010, 2010–2015, and 2015–2020), using the DSAS v 4.4 module in ArcGis 10.5 [27]. In essence, the DSAS is a GIS tool that allows the construction of equidistant transects from a baseline [28]. The fact that these transects cross the different shorelines (i.e., vectors), allowed us to estimate the statistics, such as the net movement of the coastline (m) and the rate of change (m/year). We quantified the cross-shore distance changes through sequences of the transects with a 50-m separation. Although it is beyond the scope of this article to review the accuracy of different shoreline extraction methods, the following reviews could be helpful for the reader (e.g., [15,18,29,30]). To understand the oceanographic conditions at the time we obtained the images, we extracted and calculated the wave energy and the direction data from the ERA5 dataset produced by the European Centre for Medium-Range Weather Forecast, which provided hourly ocean conditions as of January 1980 at the offshore of Mazatlan.

3. Results

The first in situ cross-shore distance and dune height at the north section of the study area (0 to 4.3 km) represents a dichotomy between a conserved region with a dune up to 8–11 m high and a cross-shore distance between 60 to 90 m (Figure 2a), with relatively recent real estate seafront constructions with seawalls in front of the foredune (Figure 2b).

The following section, which corresponds to the heavily dense resort area at the alongshore distance between 4.3 km to 8.5 km, presents beach erosion probably due to the construction of breakwaters and groins. In this sense, Figure 2c depicts a breakwater structure that has created a very narrow strip of up to 80 m on the beach. However, this type of defense array has resulted in an adjacent erosion pattern, leading to the common practice of constructing seawalls. In some locations, there is too much beach erosion, and the waves impact the resort wall directly, even at low tide (Figure 2d). Within the resort area, there is a small strip, less than 90-m wide at 8.8 km, which constitutes the only unconstructed location that shows the beach and foredune conditions as they originally were, with a maximum cross-shore distance of 90 m and a beach height of 4 m. The remaining section represented by the concrete oceanfront corridor does not display any apparent erosion (Figure 2e,f).

Figure 2. Field cross-shore distance and beach height along the northern section. The original conserved dune (**a**), seafront hotels with a hydrodynamic protective seawall (**b**), breakwater (**c**), vertical wall (**d**), and the concrete oceanfront corridor (**e**,**f**).

The south section of the study area shows different in situ cross-shore distances and dune height patterns when compared to the more developed northern region (Figure 3). A small cross-shore length of 70 m was recorded close to the groin at the entrance to the harbor (Figure 3a). We found only small individual houses 120 m from the shore within the first 2 km from the groin (Figure 3b). Overall, there are no coastal structures along the 10 km of beach, where it was possible to observe the maximum cross-shore distance (130 m) and the foredune corridor of 8 to 10 m height (Figure 3c), as well as the coconut plantations behind the foredune corridor (Figure 3d). We located only one seafront hotel in this area, at the southernmost part of the shoreline, where there is an abrupt decrease in the cross-shore distance (70 m) and in beach height (4 m).

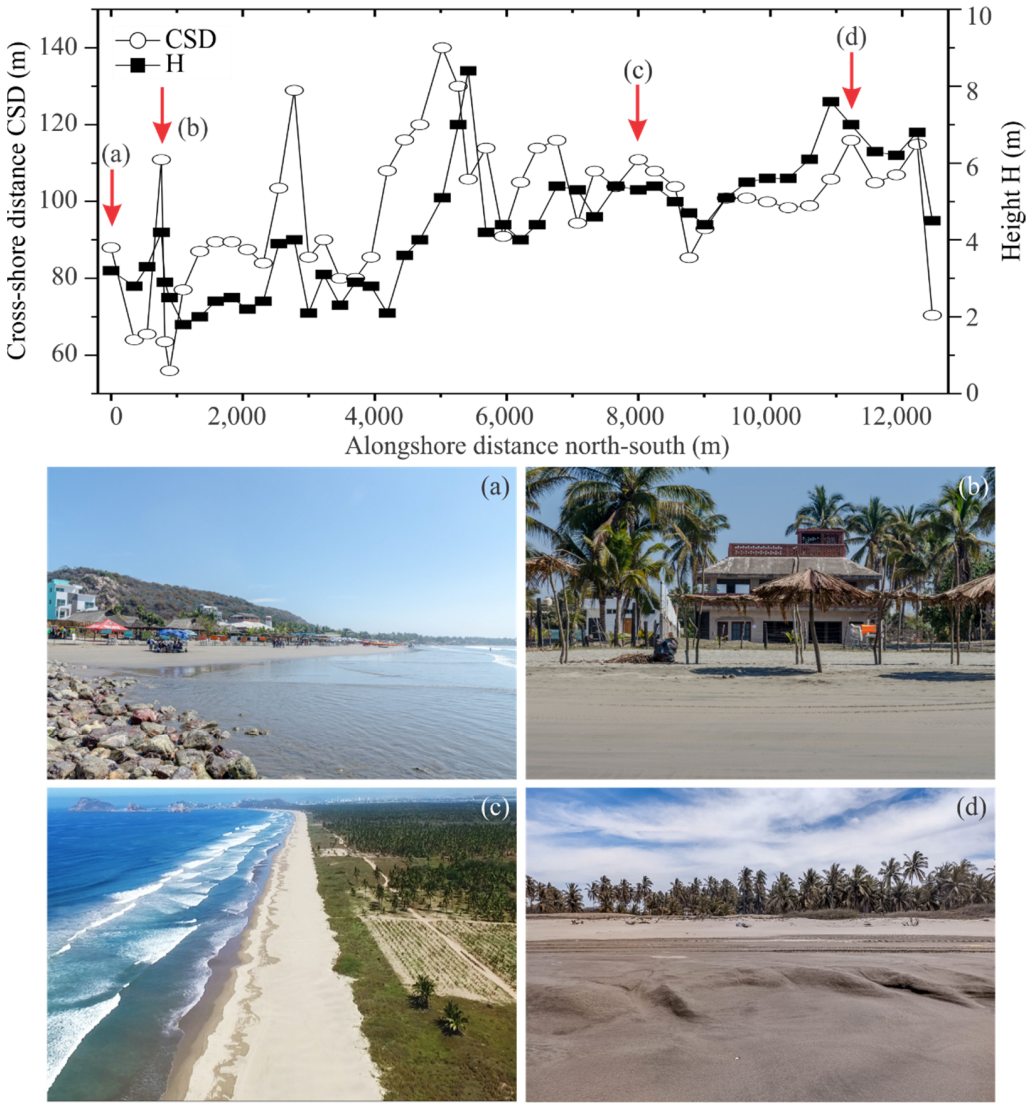

Figure 3. Field cross-shore distance and beach height along the southern section. Breakwater section in front of the harbor (**a**), one of the few structures on the beach (**b**), and the conservation area, which is unobstructed by infrastructure (**c**,**d**).

Regarding the recorded direction of the historical wave energy of the coast of Mazatlan (ERA5), the overall southwest wave pattern did not change throughout the study period (1986–2020) (Figure 4). Moreover, we detected the highest values (3.3 kJ/m^2) during hurricanes Roslyn (H1 1986), Rosa (H2 1994), Norman (H1 2000), Lane (H3 2006), Rick (H1 2009), and Willa (H3 2018).

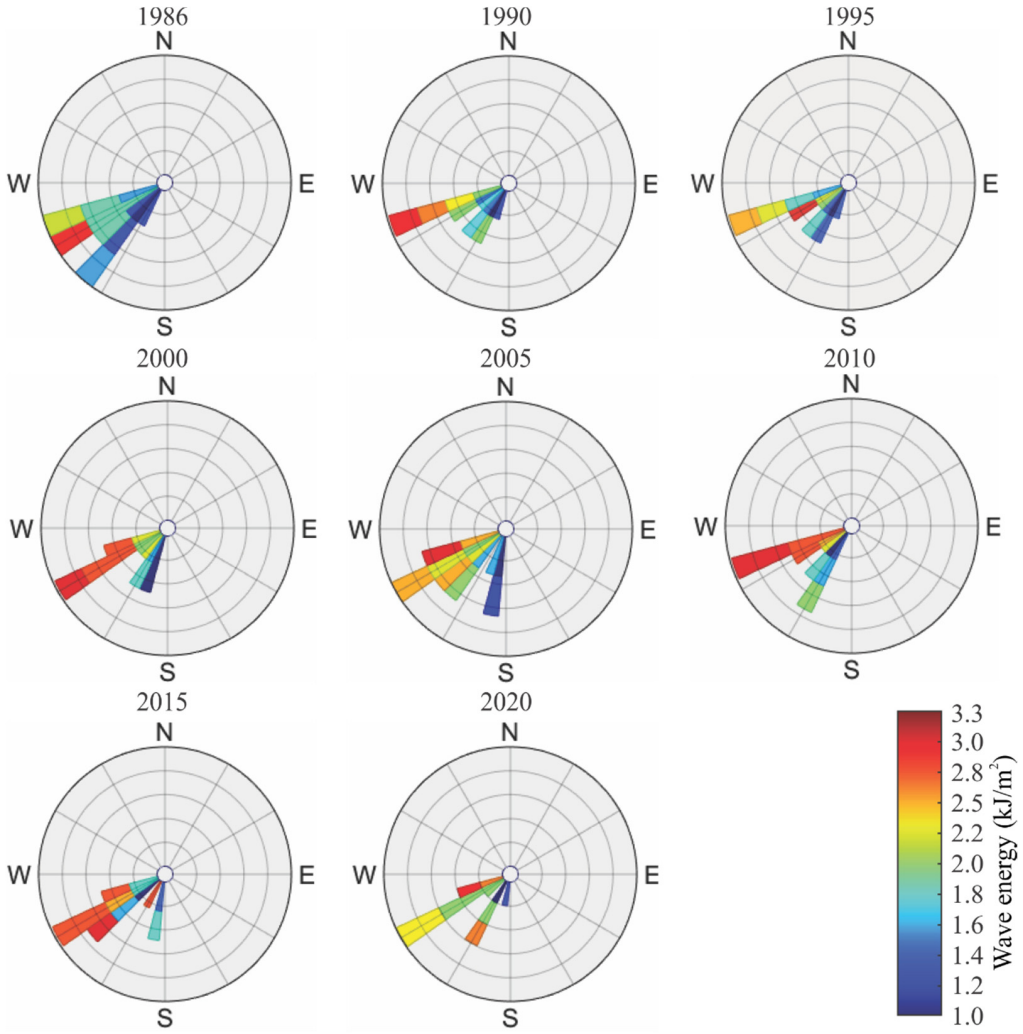

Figure 4. Historical (1986–2020) maximum wave height and direction based on the ERA5 analysis.

The RMSE of the satellite data depends largely on the spatial resolution of the sensor. However, we detected a RMSE much smaller than the Landsat spatial resolution (30 m), with a maximum of 10.2 m and a minimum of 3.8 m (Table S1). In the case of the Sentinel-2 data with a spatial resolution of 10 m, the RMSEs were sub-metric (<1 m). The estimated mean sea level at the time of the image capture varied considerably because the sensor orbits were not linked to a particular tidal range. However, the tides in this area are semi-diurnal with a relatively smaller tidal amplitude than in other regions. In this sense, the variations between the mean sea level were less than 0.4 m, with some exceptions that reached 0.7 m and −0.5 m.

In the spatial examination, corresponding to the CoastSat and DSAS analyses, we obtained 271 and 349 transects for the north and south locations, respectively. Figure 5 shows the overall cross-distance change between 1986 and 2020 (upper map) and the net cross-shore distance for the seven periods (lower graphs). The overall cross-shore distance change indicated negative values (i.e., erosive processes) recorded between transects 56–70, 125–140, and 176–190, which are in front of resort buildings. The northernmost locations (transects 56–70) show historical shoreline erosion since 2005, which agrees with the date of construction of the seafront buildings. The second section (transects 125–140) shows shoreline erosion since 2000, and in the last section (transects 176–190), there has been shoreline erosion since 1990.

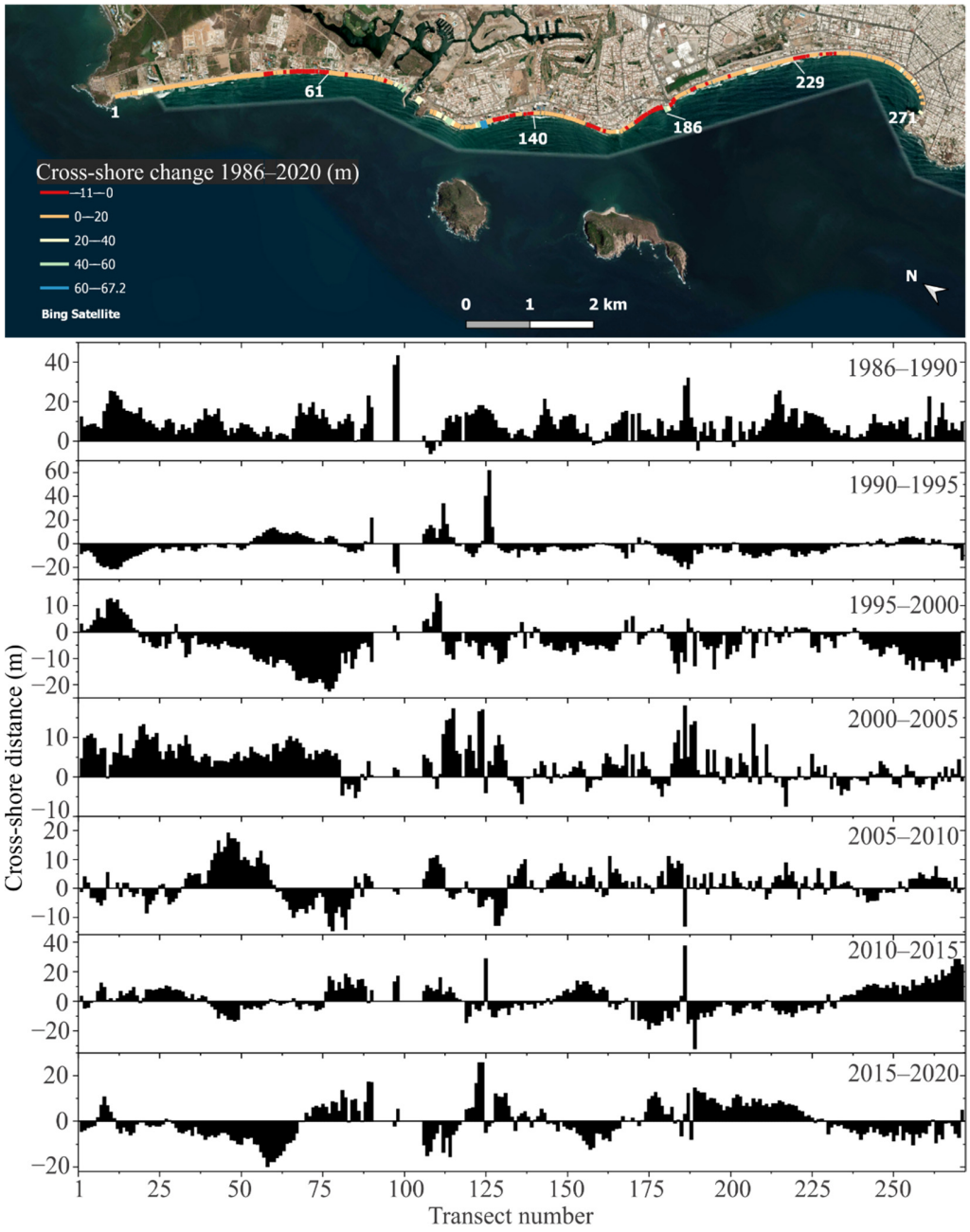

Figure 5. Across-shore distance change (1986–2020) along the coastline's northern section of the study site (**top**). Specific accretion and erosion sections among the seven periods based on the CoastSat and DSAS analyses (**bottom**). Positive values represent accretion, while negative values indicate erosion.

We recorded an interannual alternation between accretion and erosion patterns at the northernmost and southernmost regions between transects 1–40, 188–189, and 240–271, corresponding to conservation areas without infrastructure on the dune. However, we also detected other accretion areas near the breakwater and groins. This is the case of transects 89–90, 111–112, and 125–126, with accretion trends occurring in 1990–1995 and 2015–2020 (transects 89–90), 1990–1995 and 2000–2005 (transects 111–112), and 1990–1995 (transects 125–126).

Figure 6 shows the same variables as Figure 5 but in the southern section. Unlike the northern region, the transects with positive values (i.e., accretion processes) predominate in the overall balance (1986–2020), which is clear, during the 2015–2020 period. We recorded the highest cross-shore distance variability at transects 300–349, which corresponds to the

ephemeral mouth of the Presidio River. We observed the most stable shoreline conditions (neither accretion nor erosion) at transects 1–11, representing the rock formation of the harbor. There is a general accretion pattern along the coastline from 1986 to 1990, except for the first transects (11–60). This pattern also occurred in the northern, more developed region during the same period, which, at this time, presented a very low real estate oceanfront infrastructure density. The situation changed in 1990–1995 when the southern conservation region continued to show a general accretion pattern, but the northern one now shows much more erosion. In this sense, Hurricane Rosa impacted both coastlines; however, it appears that the north area was more affected.

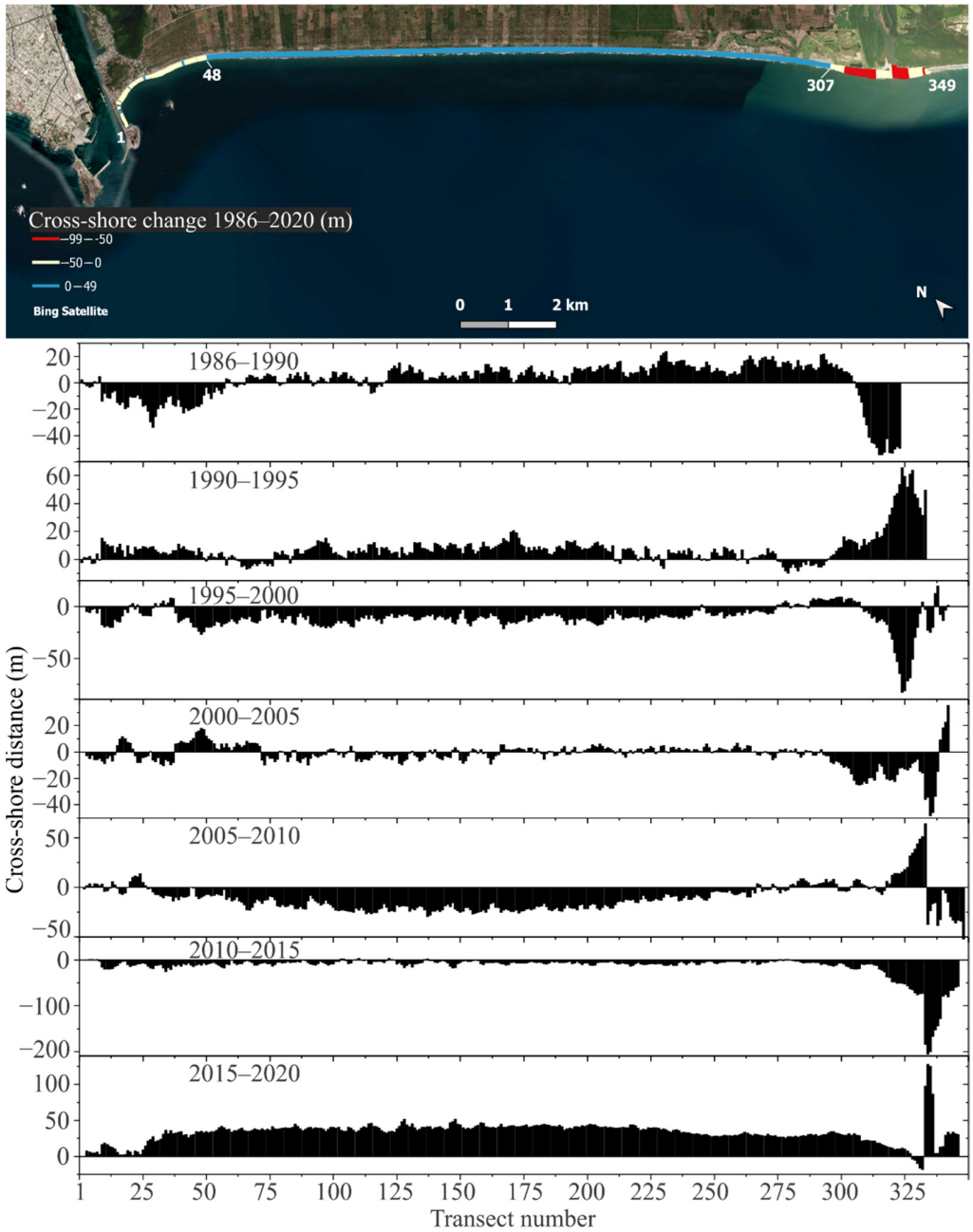

Figure 6. Across-shore distance change (1986–2020) along the coastline's southern section of the study site (**top**). Specific accretion and erosion sections among the seven periods, based on the CoastSat and DSAS analyses (**bottom**). Positive values represent accretion, while negative values indicate erosion.

4. Discussion

It is now well known that alterations in sediment transport are the main cause of shoreline erosion and ecosystem degradation, on a global scale [6]. The eastern coast of the Gulf of California is no exception. Recent studies have reported enormous shoreline loss in this region, due to anthropogenic activities, such as the construction of hydroelectric dams [31], coastal infrastructure projects [32], aquaculture [33], and the unregulated expansion of economic activities, such as coastal urbanization [1]. Unfortunately, this situation has repeated itself in many popular tourist destinations around the globe. The results of our study revealed a substantial difference in the erosion and accretion patterns along a moderately small fraction of the coastline (26 km), but with contrasting shoreline characteristics. We found that the major causes of the historical erosion along the tourist city of Mazatlan are a combination of unplanned real estate construction facing the beach, the foredune and beach berm fragmentation, and the intensity and direction of the swell from tropical storms and hurricanes.

The southern shoreline section of Mazatlan is a clear example of beach conservation, mainly because there has been no coastal infrastructure development yet. Over the last three decades, the overall change in the cross-shore distance has led to a constant accretion of 50 to 70 m of sandy beach. This historical pattern agrees with the field survey, providing on-site information about the original foredune and beach berm conditions with a maximum cross-shoreline distance of up to 130 m and a dune height of 8 to 10 m. These results are disparate, compared to the beach conditions near the harbor groin because these defensive coastal structures are associated with erosive processes by reducing the littoral transport of sediments [34].

Concerning the shoreline evolution surrounding the Presidio River mouth, the oceanfront resort has decreased the cross-shore extension and dune height. Still, we did not record excessive beach erosion at this location. The lack of shoreline erosion may be associated with the proximity to the sediment plume from the river, with an average annual discharge of 1162 million m^3 during the rainy season [35]. However, this pattern could have changed far from the river mouth because it may not be directly related to the river's influence. The river mouth presents a huge shoreline variability between erosion and accretion trends, due to its forceful fluvial currents during the rainy season. Interestingly, the riparian vegetation of the Presidio River consists of a dense mangrove forest that promotes the exportation of organic matter into the coastline [36].

Given that the coastal development started during the last two decades in the northernmost region, there is a marked contrast between the unobstructed foredune and beach berm, compared with oceanfront resorts. The results of the field surveys and the spatial analysis indicated that accretion areas of the beach are found in front of unobstructed sections with cross-shore distances of 60 to 90 m and dune heights of 8 to 10 m, just as the southernmost conserved coastal zone. Not surprisingly, previous studies have indicated a direct relationship between the size of the foredune and the beach extension due to sediment transport [7,14]. Hence, conserving the corridor between the foredune and the beach berm is of utmost importance for beach management and preservation [5].

Coastal dunes form a protective barrier and are relevant during extreme erosion events, such as swelling under hurricane conditions [37]. This particular characteristic could be of critical importance along the Mazatlan coastline, which does not have a natural defense against waves, such as coral reef barriers. There are two islands in front of the tourist zone where the highest density of the oceanfront structures is presented. These islands are expected to form a natural protective barrier against the waves, especially during storm events. Although there are no wave refraction and diffraction studies in this area, the waves are expected to decrease their energy in coastal regions facing the islands and increase their energy at the sides based on the angle of incidence and the bathymetry. However, in situ and remote sensing data indicate that the coastline facing the south island area shows maximum erosion. A possible solution could be constructing underwater structures (i.e., similar to coral reefs) in front but not in direct contact with

the most eroded areas—however, this endeavor will require accurate coastal circulation models, government permits, and substantial investment.

The people involved in decision-making must analyze and select the attributes to address the specific concerns and follow the best course of action [37]. In this sense, the results of our analysis stress the need to include in situ and spatial analysis techniques as complementary tools in coastal monitoring programs. For instance, the variations in the shoreline position since 1990 indicate that the city of Mazatlan has constantly been undergoing shoreline erosion at some locations. The only sediment supply in this area corresponds to the sand distribution by the littoral current, which has a velocity of 1 to 5 cm s^{-1} and a predominance towards the north during most of the year [35]. Unfortunately, although a series of rigid defensive structures, such as groins and breakwaters, have been constructed to preserve the beach, these structures still cause substantial changes in sediment transport [38], exacerbating shoreline erosion according to the direction of the current.

Despite the shoreline damage due to the presence of unplanned rigid defensive structures, external factors, such as the sea-level rise, the obstruction of rivers, and the frequency of extreme ocean-meteorological events, such as hurricanes, may exacerbate erosion processes ([36,39]). The sea-level rise in the Gulf of California has a geographical gradient of 2.5 mm $year^{-1}$ at the gulf's entrance [11]. However, we believe that the increase in the intensity and frequency of hurricanes in the coming decades will substantially impact coastal erosion and overall shoreline dynamics in this study area ([40,41]). The historical maximum wave energy and the constant direction from the southwest are clear indicators of the presence of hurricanes in this region. Moreover, the Easter coast of the Gulf of California has been more vulnerable to the effects of storm surge elevation because of the topographic slope (collision coast) and the apparent increase of wave energy during the last decades [11]. These events could cause severe beach erosion, as observed with the recent impact of hurricane Nora (H1) on 29 August 2021. A hurricane category 3 to 5 will be able to exacerbate the flooding and overall coastal damage.

The city of Mazatlan, as well as many other popular tourist destinations, does not have a long-term monitoring program regarding beach management. This is why digital shoreline mapping that spans different decades is the only alternative approach capable of providing a comprehensive aspect of the shoreline evolution. Using satellite data and novel processing techniques, such as CoastSat, have allowed us to analyze vast amounts of spatial data efficiently. The historical spatial results of our study area are in accordance with the in situ observations. This is why we believe our method is robust and provides essential information regarding sandy beach management. The use of multi-temporal Landsat data with DSAS has been a practical approach for historical shoreline variability along sections of the Gulf of California ([31,32]) and other study sites (e.g., [6,14,17,42]).

Nonetheless, and as far as we are concerned, only a few recent studies have used the CoastSat platform [24]. Therefore, it is clear that this technology will continue to advance in the coming years, increasing the possibility of novel satellite acquisition sensors and spatial approaches. For instance, it is now possible to acquire freely available multispectral images at a 10-m spatial resolution with a temporal resolution of five days—an unheard-of situation before 2018. We believe that very-high spatial resolution satellite data (<4 m) will be freely available in the future, and that this will improve the shoreline detection accuracy.

Researchers can replicate the method used in this study in other popular tourist destinations around the world that have a certain degree of coastal degradation. For instance, the causes of coastal erosion are repeated everywhere when the expansion of real estate tourist infrastructure and coastal defensive constructions are unplanned. Although this situation has been known for many decades, it continues, nonetheless. Despite the favorable results of our analysis, persistent cloud cover can be a hindrance when using passive remote sensing data, as also happens with the sensor's pixel size when using multi-platforms in tidal environments [43]. However, the results of the in situ shoreline survey are consistent with the historical spatial analysis of the shoreline evolution.

5. Conclusions

This study implemented a series of analyses involving in situ topographic surveys and a freely available cloud computing approach (CoastSat) along the coastline of Mazatlan from 1986 to 2020. The tourist city of Mazatlan in Mexico reflects a typical pattern within the coastal cities of Latin America, where unplanned real estate oceanfront developments and coastal defensive constructions tend to decrease the beach value by increasing the shoreline erosion. The results highlight the direct relationship between the cross-shore distance and dune height from the field survey with the accretion and erosion patterns derived from the multi-decadal analysis of the CoastSat data. The shoreline region with a dense real estate oceanfront infrastructure presents a minimum cross-shore distance of 0 to 10 m and a beach height of less than 2 m. Although some resorts are currently under direct impact by waves, it has been possible to detect very few unobstructed sections in the same area with the original foredune and beach, exhibiting a notable difference with the cross-shore distance between 60 to 90 m and the dune height between 8 to 10 m. The conservation area (southern region), located on the other side of the harbor entrance, shows maximum cross-shore distances of 130 m and dune heights of 8 to 10 m. As we have implemented a successful multi-method assessment in Mexico, this synergetic approach could be applied to any part of the World where coastal survey programs do not exist. In fact, with the ongoing global development of real estate and harbors, there is a pressing need for additional research that will consider long-term data for monitoring coastal systems using in situ and remote sensing data. We thus hope this work will create awareness about the reality of coastal erosion by fragmenting the foredune and beach berm. This will be particularly important in the southern section of the study area, where a recent interest in the development of major oceanfront resorts is emerging.

Supplementary Materials: The following information can be downloaded at: https://www.mdpi.com/article/10.3390/geographies2040039/s1, Table S1: Remote sensing data collected from the CoastSat analysis.

Author Contributions: Conceptualization, L.V.-L. and F.F.-d.-S.; methodology, F.F.-d.-S.; software, L.V.-L.; validation, F.F.-V. and F.F.-d.-S.; formal analysis, L.V.-L.; investigation, L.V.-L.; resources, F.F.-d.-S.; data curation, L.V.-L.; writing—original draft preparation, F.F.-d.-S.; writing—review and editing, F.F.-d.-S., L.V.-L. and F.F.-V.; visualization, F.F.-d.-S.; supervision, F.F.-V.; project administration, F.F.-d.-S.; funding acquisition, F.F.-d.-S. All authors have read and agreed to the published version of the manuscript.

Funding: This research was funded by the Programa de Apoyo a Proyectos de Investigación e Innnovación Tecnológica (PAPIIT), grant number IA100521, and the Instituto de Ciencias del Mar y Limnología (UNAM), grant number 323.

Data Availability Statement: This data can be found at UNINMAR: http://www.icmyl.unam.mx/uninmar/ (accessed on 31 August 2022).

Acknowledgments: Many thanks to Guillermina Feher for reviewing the English text. Ocean. Bruno Matteotti Sánchez provided the bathymetric data.

Conflicts of Interest: The authors declare no conflict of interest.

References

1. Burt, J.A.; Killilea, M.E.; Ciprut, S. Coastal Urbanization and Environmental Change: Opportunities for Collaborative Education across a Global Network University. *Reg. Stud. Mar. Sci.* **2019**, *26*, 100501. [CrossRef]
2. Lausch, A.; Pause, M.; Merbach, I.; Zacharias, S.; Doktor, D.; Volk, M.; Seppelt, R. A New Multiscale Approach for Monitoring Vegetation Using Remote Sensing-Based Indicators in Laboratory, Field, and Landscape. *Environ. Monit. Assess.* **2013**, *185*, 1215–1235. [CrossRef] [PubMed]
3. Melet, A.; Teatini, P.; le Cozannet, G.; Jamet, C.; Conversi, A.; Benveniste, J.; Almar, R. Earth Observations for Monitoring Marine Coastal Hazards and Their Drivers. *Surv. Geophys.* **2020**, *41*, 1489–1534. [CrossRef]
4. Perkins, M.J.; Ng, T.P.T.; Dudgeon, D.; Bonebrake, T.C.; Leung, K.M.Y. Conserving Intertidal Habitats: What Is the Potential of Ecological Engineering to Mitigate Impacts of Coastal Structures? *Estuar. Coast. Shelf Sci.* **2015**, *167*, 504–515. [CrossRef]

5. Feagin, R.A.; Figlus, J.; Zinnert, J.C.; Sigren, J.; Martínez, M.L.; Silva, R.; Smith, W.K.; Cox, D.; Young, D.R.; Carter, G. Going with the Flow or against the Grain? The Promise of Vegetation for Protecting Beaches, Dunes, and Barrier Islands from Erosion. *Front. Ecol. Environ.* **2015**, *13*, 203–210. [CrossRef]
6. Lausch, A.; Schaepman, M.E.; Skidmore, A.K.; Truckenbrodt, S.C.; Hacker, J.M.; Baade, J.; Bannehr, L.; Borg, E.; Bumberger, J.; Dietrich, P.; et al. Linking the Remote Sensing of Geodiversity and Traits Relevant to Biodiversity—Part II: Geomorphology, Terrain and Surfaces. *Remote Sens.* **2020**, *12*, 3690. [CrossRef]
7. Kombiadou, K.; Costas, S.; Carrasco, A.R.; Plomaritis, T.A.; Ferreira, Ó.; Matias, A. Bridging the Gap between Resilience and Geomorphology of Complex Coastal Systems. *Earth-Sci. Rev.* **2019**, *198*, 102934. [CrossRef]
8. Ranasinghe, R. Assessing Climate Change Impacts on Open Sandy Coasts: A Review. *Earth-Sci. Rev.* **2016**, *160*, 320–332. [CrossRef]
9. Williams, A.T.; Rangel-Buitrago, N.; Pranzini, E.; Anfuso, G. The Management of Coastal Erosion. *Ocean Coast. Manag.* **2018**, *156*, 4–20. [CrossRef]
10. Łabuz, T.A. A Review of Field Methods to Survey Coastal Dunes—Experience Based on Research from South Baltic Coast. *J. Coast. Conserv.* **2016**, *20*, 175–190. [CrossRef]
11. Franco-Ochoa, C.; Zambrano-Medina, Y.; Plata-Rocha, W.; Monjardín-Armenta, S.; Rodríguez-Cueto, Y.; Escudero, M.; Mendoza, E. Long-Term Analysis of Wave Climate and Shoreline Change along the Gulf of California. *Appl. Sci.* **2020**, *10*, 8719. [CrossRef]
12. Powell, E.J.; Tyrrell, M.C.; Milliken, A.; Tirpak, J.M.; Staudinger, M.D. A Review of Coastal Management Approaches to Support the Integration of Ecological and Human Community Planning for Climate Change. *J. Coast. Conserv.* **2019**, *23*, 1–18. [CrossRef]
13. Eichentopf, S.; Karunarathna, H.; Alsina, J.M. Morphodynamics of Sandy Beaches under the Influence of Storm Sequences: Current Research Status and Future Needs. *Water Sci. Eng.* **2019**, *12*, 221–234. [CrossRef]
14. de Oliveira, J.F.; Barboza, E.G.; Martins, E.M.; Scarelli, F.M. Geomorphological and Stratigraphic Analysis Applied to Coastal Management. *J. S. Am. Earth Sci.* **2019**, *96*, 102358. [CrossRef]
15. Boak, E.H.; Turner, I.L. Shoreline Definition and Detection: A Review. *J. Coast. Res.* **2005**, *214*, 688–703. [CrossRef]
16. Gonçalves, R.M.; Saleem, A.; Queiroz, H.A.A.; Awange, J.L. A Fuzzy Model Integrating Shoreline Changes, NDVI and Settlement Influences for Coastal Zone Human Impact Classification. *Appl. Geogr.* **2019**, *113*, 102093. [CrossRef]
17. Apostolopoulos, D.N.; Nikolakopoulos, K.G. Assessment and Quantification of the Accuracy of Low- and High-Resolution Remote Sensing Data for Shoreline Monitoring. *ISPRS Int. J. Geo-Inf.* **2020**, *9*, 391. [CrossRef]
18. Román-Rivera, M.A.; Ellis, J.T. A Synthetic Review of Remote Sensing Applications to Detect Nearshore Bars. *Mar. Geol.* **2019**, *408*, 144–153. [CrossRef]
19. Nazeer, M.; Waqas, M.; Shahzad, M.I.; Zia, I.; Wu, W. Coastline Vulnerability Assessment through Landsat and Cubesats in a Coastal Mega City. *Remote Sens.* **2020**, *12*, 749. [CrossRef]
20. Purkis, S.J.; Gardiner, R.; Johnston, M.W.; Sheppard, C.R.C. A Half-Century of Coastline Change in Diego Garcia–The Largest Atoll Island in the Chagos. *Geomorphology* **2016**, *261*, 282–298. [CrossRef]
21. Cellone, F.; Carol, E.; Tosi, L. Coastal Erosion and Loss of Wetlands in the Middle Río de La Plata Estuary (Argentina). *Appl. Geogr.* **2016**, *76*, 37–48. [CrossRef]
22. INEGI. *Anuario Estadístico del Estado de Sinaloa*; INEGI: Ciudad de México, Mexico, 2018.
23. Brito-Rodríguez, M.; Cánoves-Valiente, G. Tourism Development in Mazatlan, Mexico: An Analysis of the Conditions of Sustainability. *Cuad. Tur.* **2019**, *43*, 579–583.
24. Vos, K.; Splinter, K.D.; Harley, M.D.; Simmons, J.A.; Turner, I.L. CoastSat: A Google Earth Engine-Enabled Python Toolkit to Extract Shorelines from Publicly Available Satellite Imagery. *Environ. Model. Softw.* **2019**, *122*, 104528. [CrossRef]
25. Vos, K.; Harley, M.D.; Splinter, K.D.; Simmons, J.A.; Turner, I.L. Sub-Annual to Multi-Decadal Shoreline Variability from Publicly Available Satellite Imagery. *Coast. Eng.* **2019**, *150*, 160–174. [CrossRef]
26. Lennert, M. Addon. v.Centerline.Py 2017. Available online: https://grass.osgeo.org/grass78/manuals/addons/v.centerline.html (accessed on 1 March 2021).
27. Thieler, E.R.; Danforth, W.W. Historical Shoreline Mapping (II): Application of the Digital Shoreline Mapping and Analysis Systems (DSMS/DSAS) to Shoreline Change Mapping in Puerto Rico. *J. Coast. Res.* **1994**, *10*, 600–620.
28. Bheeroo, R.A.; Chandrasekar, N.; Kaliraj, S.; Magesh, N.S. Shoreline Change Rate and Erosion Risk Assessment along the Trou Aux Biches–Mont Choisy Beach on the Northwest Coast of Mauritius Using GIS-DSAS Technique. *Environ. Earth Sci.* **2016**, *75*, 444. [CrossRef]
29. Gens, R. Remote Sensing of Coastlines: Detection, Extraction and Monitoring. *Int. J. Remote Sens.* **2010**, *31*, 1819–1836. [CrossRef]
30. Nel, R.; Campbell, E.E.; Harris, L.; Hauser, L.; Schoeman, D.S.; McLachlan, A.; du Preez, D.R.; Bezuidenhout, K.; Schlacher, T.A. The Status of Sandy Beach Science: Past Trends, Progress, and Possible Futures. *Estuar. Coast. Shelf Sci.* **2014**, *150*, 1–10. [CrossRef]
31. Valderrama-Landeros, L.; Flores-de-Santiago, F. Assessing Coastal Erosion and Accretion Trends along Two Contrasting Subtropical Rivers Based on Remote Sensing Data. *Ocean Coast. Manag.* **2019**, *169*, 58–67. [CrossRef]
32. Valderrama-Landeros, L.; Blanco y Correa, M.; Flores-Verdugo, F.; Álvarez-Sánchez, L.F.; Flores-de-Santiago, F. Spatiotemporal Shoreline Dynamics of Marismas Nacionales, Pacific Coast of Mexico, Based on a Remote Sensing and GIS Mapping Approach. *Environ. Monit. Assess.* **2020**, *192*, 123. [CrossRef] [PubMed]

33. Serrano, D.; Flores-Verdugo, F.; Ramírez-Félix, E.; Kovacs, J.M.; Flores-de-Santiago, F. Modeling Tidal Hydrodynamic Changes Induced by the Opening of an Artificial Inlet within a Subtropical Mangrove Dominated Estuary. *Wetl. Ecol. Manag.* **2020**, *28*, 103–118. [CrossRef]
34. Jiménez-Illescas, Á.R.; Zayas-Esquer, M.M.; Espinosa-Carreón, T.L. Integral Management of the Coastal Zone to Solve the Problems of Erosion in Las Glorias Beach, Guasave, Sinaloa, Mexico. In *Coastal Management*; Elsevier: Amsterdam, The Netherlands, 2019; pp. 141–163.
35. Serrano, D.; Valle-Levinson, A. Effects of River Discharge and the California Current on Pycnocline Depth at the Eastern Entrance to the Gulf of California. *Cont. Shelf Res.* **2021**, *215*, 104356. [CrossRef]
36. Vizcaya-Martínez, D.A.; Flores-de-Santiago, F.; Valderrama-Landeros, L.; Serrano, D.; Rodríguez-Sobreyra, R.; Álvarez-Sánchez, L.F.; Flores-Verdugo, F. Monitoring Detailed Mangrove Hurricane Damage and Early Recovery Using Multisource Remote Sensing Data. *J. Environ. Manag.* **2022**, *320*, 115830. [CrossRef] [PubMed]
37. Schlacher, T.A.; Schoeman, D.S.; Jones, A.R.; Dugan, J.E.; Hubbard, D.M.; Defeo, O.; Peterson, C.H.; Weston, M.A.; Maslo, B.; Olds, A.D.; et al. Metrics to Assess Ecological Condition, Change, and Impacts in Sandy Beach Ecosystems. *J. Environ. Manag.* **2014**, *144*, 322–335. [CrossRef] [PubMed]
38. García-Rubio, G.; Huntley, D.; Russell, P. Evaluating Shoreline Identification Using Optical Satellite Images. *Mar. Geol.* **2015**, *359*, 96–105. [CrossRef]
39. Dean, R.G.; Houston, J.R. Determining Shoreline Response to Sea Level Rise. *Coast. Eng.* **2016**, *114*, 1–8. [CrossRef]
40. Han, X.; Feng, L.; Hu, C.; Kramer, P. Hurricane-Induced Changes in the Everglades National Park Mangrove Forest: Landsat Observations Between 1985 and 2017. *J. Geophys. Res. Biogeosc.* **2018**, *123*, 3470–3488. [CrossRef]
41. Montgomery, J.M.; Bryan, K.R.; Mullarney, J.C.; Horstman, E.M. Attenuation of Storm Surges by Coastal Mangroves. *Geophys. Res. Lett.* **2019**, *46*, 2680–2689. [CrossRef]
42. Godwyn-Paulson, P.; Jonathan, M.P.; Roy, P.D.; Rodríguez-Espinosa, P.F.; Muthusankar, G.; Muñoz-Sevilla, N.P.; Lakshumanan, C. Evolution of Southern Mexican Pacific Coastline: Responses to Meteo-Oceanographic and Physiographic Conditions. *Reg. Stud. Mar. Sci.* **2021**, *47*, 101914. [CrossRef]
43. Xu, C.; Liu, W. The Spatiotemporal Characteristics and Dynamic Changes of Tidal Flats in Florida from 1984 to 2020. *Geographies* **2021**, *1*, 292–314. [CrossRef]